Taxol Binds to Polymerized Tubulin In Vitro

JEROME PARNESS and SUSAN BAND HORWITZ
Departments of Molecular Pharmacology and Cell Biology, Albert Einstein College of Medicine, Bronx, New York 10461

ABSTRACT Taxol, a natural plant product that enhances the rate and extent of microtubule assembly in vitro and stabilizes microtubules in vitro and in cells, was labeled with tritium by catalytic exchange with ^3H_2O. The binding of [^{3}H]taxol to microtubule protein was studied by a sedimentation assay. Microtubules assembled in the presence of [^{3}H]taxol bind drug specifically with an apparent binding constant, K_{app}, of 8.7×10^{-7} M and binding saturates with a calculated maximal binding ratio, B_{max}, of 0.6 mol taxol bound/mol tubulin dimer. [^{3}H]Taxol also binds and assembles phosphocellulose-purified tubulin, and we suggest that taxol stabilizes interactions between dimers that lead to microtubule polymer formation. With both microtubule protein and phosphocellulose-purified tubulin, binding saturation occurs at approximate stoichiometry with the tubulin dimer concentration. Under assembly conditions, podophyllotoxin and vinblastine inhibit the binding of [^{3}H]taxol to microtubule protein in a complex manner which we believe reflects a competition between these drugs, not for a single binding site, but for different forms (dimer and polymer) of tubulin. Steady-state microtubules assembled with GTP or with 5′-guanylyl-α,β-methylene diphosphonate (GPCPP), a GTP analog reported to inhibit microtubule treadmilling (I. V. Sandoval and K. Weber. 1980. *J. Biol. Chem.* 255:6966–6974), bind [^{3}H]taxol with approximately the same stoichiometry as microtubules assembled in the presence of [^{3}H]taxol. Such data indicate that a taxol binding site exists on the intact microtubule. Unlabeled taxol competitively displaces [^{3}H]taxol from microtubules, while podophyllotoxin, vinblastine, and $CaCl_2$ do not. Podophyllotoxin and vinblastine, however, reduce the mass of sedimented taxol-stabilized microtubules, but the specific activity of bound [^{3}H]taxol in the pellet remains constant. We conclude that taxol binds specifically and reversibly to a polymerized form of tubulin with a stoichiometry approaching unity.

Of the plant products known to interact with microtubule protein (MTP), taxol, an experimental antitumor agent isolated from *Taxus brevifolia* (1), is the only one that has been reported to promote microtubule (MT) assembly. Taxol enhances both the rate and extent of in vitro calf-brain MTP assembly in the presence or absence of exogenous GTP, and stabilizes those MTs to depolymerization by cold treatment (4°C) and $CaCl_2$ (4 mM). Similar results are observed with taxol and phosphocellulose-purified tubulin in the presence of GTP. The effects of taxol on the rate and yield of MT formation have been related to an increase in the number of MT nucleation events. This is manifested by a decrease both in the mean MT length and in the critical concentration of MTP required for assembly: events that are concomitant with an increase in the yield of sedimented MTs. It also has been demonstrated that taxol stabilizes assembled MTs, implying that a taxol binding site(s) exists on the formed polymer. Maximum effects of the drug are seen at concentrations stoichiometric with the tubulin dimer concentration (2, 3, 4). Experiments done in cell culture have shown that taxol stabilizes MTs in BALB/c fibroblasts to depolymerization by cold treatment and by steganacin, an inhibitor of MT assembly (5). These results suggest that taxol interacts with tubulin to induce the formation and enhance the stability of MTs in cells as well as in vitro.

To directly assess the association of taxol with tubulin both in vitro and in cells, we prepared tritium-labeled drug. We report here the characterization of the in vitro binding of [^{3}H]taxol to calf-brain MTP. Taxol binding to tubulin polymer was studied by a sedimentation assay and the use of MT assembly inhibitors. Electron microscopy was used to correlate taxol binding with polymer morphology.

MATERIALS AND METHODS

Preparation of Microtubule Protein

Calf-brain MTP was purified through two cycles of temperature-dependent assembly-disassembly by the method of Shelanski et al. (6) and was stored in

THE JOURNAL OF CELL BIOLOGY · VOLUME 91 NOVEMBER 1981 479-487

liquid N_2 as 1- to 2-ml aliquots made 1 mM in GTP and 4 M in glycerol. Before each experiment, MTP was dialyzed with 100 vol of MES buffer (0.1 M 2-[N-morpholino]ethanesulfonic acid [MES], 1 mM EGTA, 0.5 mM $MgCl_2$ adjusted to pH 6.6 with NaOH) for 3 h at 4°C and centrifuged at 120,000 *g* for 20 min at 4 °C. The supernate was kept at 4°C and used within 1 h of centrifugation.

To determine the purity of tubulin in these preparations, increasing concentrations of MTP (8–80 μg) were run on 8% SDS polyacrylamide slab gels (7), stained with Coomassie Blue and, after destaining, scanned at 600 nm on an RFT scanning densitometer (Transidyne General Corp., Ann Arbor, Mich.). Tubulin purity averaged 70 ± 10%, and this value was used for all calculations reported in the text. The molecular weight of tubulin was taken as 110,000 (8). As has been previously reported (9, 10), neurofilaments were a contaminant in all preparations and were seen in electron micrographs and on SDS polyacrylamide gels.

Purified tubulin was prepared from twice-cycled calf-brain MTP by chromatography on phosphocellulose, according to the method of Weingarten et al. (11) and used immediately. This purified tubulin (PC-tubulin) showed no detectable Coomassie Blue–stained bands other than α- and β-tubulin on overloaded 8% SDS polyacrylamide gels.

Preparation and Purification of [^{3}H]Taxol

Taxol (obtained from the National Cancer Institute, Bethesda, Md.) was tritiated by Amersham Corp. (Arlington Heights, Ill.), using a catalytic exchange method, the conditions for which were developed in our laboratory. Taxol (25 mg) was dissolved in 0.5 ml of peroxide-free, dry dioxane to which was added 25 μl of ^3H_2O (25 Ci at ≥90% isotopic purity). This solution was placed in a sealed tube *in vacuo* containing 25 mg of rhodium on alumina powder and heated at 80°C for five h. The reaction vessel was cooled, the solvent evaporated, and the remaining material dissolved in CH_3OH. Evaporation and dissolution in CH_3OH was repeated at least three times to remove all traces of dioxane and exchangeable tritium.

[^{3}H]Taxol was purified by preparative silica-gel thin-layer chromatography. Approximately 6 mg (~10 mCi) of reaction product in 200 μl of CH_3OH was spotted across a 20 × 20 cm silica-gel TLC plate (silica-gel 60 F254, 0.25-mm thickness, E. Merck Co., Rahway, N. J.), air-dried, and developed in $CHCl_3$:CH_3OH (95:5 vol/vol) to a distance of 10 cm. The plate was air-dried and bands were visualized with UV light. Five distinct fluorescence quenching bands were visible and the most prominent, band 3 (R_f = 0.33–0.41, see below), was excised and extracted five times with 10 ml of isopropanol.[1] The isopropanol extracts were pooled, evaporated under vacuum, and the putative [^{3}H]taxol was dissolved in 1 ml of CH_3OH (Burdick and Jackson Laboratories Inc., Hoffman-LaRoche, Inc., Muskegon, Mich.). The tritiated material was evaporated and redissolved four times in CH_3OH to remove all traces of isopropanol.

Purity was determined by analytical thin-layer chromatography. Typically, 5 μl of 10^{-6} M [^{3}H]taxol in CH_3OH was mixed with 20 μl of 10^{-2} M unlabeled taxol in CH_3OH. 5 μl of this mixture was spotted on a 5 × 20 cm silica-gel plate (silica-gel 60 F254, 0.25-mm thickness), air-dried, and developed in $CHCl_3$:CH_3OH (96.5:3.5; 95:5; or 92.5:7.5, vol/vol). Taxol was visualized with UV light, and under these conditions the drug migrates with an R_f of 0.28, 0.4, and 0.48, respectively. 5-mm sections were scraped into vials and counted in 10 ml of Aquasol (New England Nuclear, Boston, Mass.). In each case, a single radioactive peak co-chromatographed with authentic taxol. [^{3}H]Taxol was estimated to be ≥98% pure. The concentration of [^{3}H]taxol was determined spectrophotometrically in CH_3OH using an extinction coefficient, ϵ_{227} of 29,800 (1), and a specific activity of 442.8 mCi/mmol was determined. [^{3}H]Taxol was diluted to various concentrations with CH_3OH and stored at −20°C. No radiochemical decomposition has been detected during six months. [^{3}H]Taxol retained complete biological activity.

[^{3}H]Taxol Binding to MTP

A sedimentation assay, the protocol for which is described below, was used to correlate the presence of labeled taxol with MTs. [^{3}H]Taxol, in the presence or absence of other drugs, 1 mM GTP or 1 mM GPCPP (ICN Nutritional Biochemicals, Cleveland, Ohio), was incubated with 0.38–0.51 mg/ml MTP or PC-tubulin in MES buffer at 37°C for 60 min in a total volume of 500 μl. After 60 min, the reaction mixture was layered on 4.5 ml of deaerated 50% sucrose in MES buffer at 25°C and centrifuged in an SW50.1 rotor in a Beckman L265B ultracentrifuge (Beckman Instruments, Inc., Spinco Div., Palo Alto, Calif.) at 230,000 *g* for 2 h at 25°C (12). After the supernatant was aspirated, the pellet was washed three times at room temperature with 70% sucrose in MES buffer and resuspended in 0.5 ml of MES buffer by sonication for 15 min in an ultrasonic bath (Heat Systems–Ultrasonics, Inc., Plainview, N. Y.). Protein concentration and radioactivity were determined in duplicate for each sample.

Protein was determined according to the method of Bradford (13) using the microassay described by Bio-Rad Laboratories (Richmond, Calif.). It was found that the MTP used in these studies bound dye in a linear fashion to ~0.6 OD at 595 nm. Determination of MTP concentration by the above method using bovine serum albumin (BSA) as a protein standard gave results almost identical to those obtained with the method of Lowry et al. (14), as modified by Bensadoun and Weinstein (15), using the same standard. Therefore, BSA was used for calibration throughout this study.

Radioactivity was determined by counting aliquots in 10 ml Aquasol in an Intertechnique Model SL4000 liquid scintillation counter (Intertechnique, Plaisir, France). Efficiency of tritium counting was ~45%.

[^{3}H]Taxol Binding to Assembled Microtubules

MTP (0.5–1 mg/ml) was incubated under assembly conditions (MES buffer, 1 mM GTP or 1 mM GPCPP, 37°C) until MT assembly reached steady-state (~30 min). Then one or two procedures was followed: (*a*) MTs were harvested by centriguation at 39,000 *g*, 25°C, for 30 min (16) and resuspended in 500 μl of MES buffer containing [^{3}H]taxol, 1 mM GTP or GPCPP, and other drugs as indicated. The resuspended MTs were incubated for an additional 30 min at 37°C, layered on 4.5 ml of 50% sucrose, and processed as described above for the sedimentation assay. (*b*) [^{3}H]Taxol and other drugs were added directly to the solution containing the assembled MTs and incubated for an additional 30 min at 37°C. 500 μl was layered on 4.5 ml of 50% sucrose and processed as described above.

Other drugs used in these assays were podophyllotoxin (Aldrich Chemical Co., Milwaukee, Wisc.), vinblastine sulfate (Sigma Chemical Co., St. Louis, Mo.) and VP-16-213 (Sandoz Pharmaceutical, Hanover, N. J.).

Electron Microscopy

5 or 10 μl of a reaction mixture was placed on carbon-over-Parlodion-coated grids (200- or 300-mesh) and negatively stained with 2% uranyl acetate. Grids were air-dried and viewed under a JEOL 100CX electron microscope at 80 kV.

Actin Polymerization

Polymerization of purified rabbit muscle actin (a gift of Dr. John Condeelis, A. Einstein College of Medicine) was followed by viscometry and electron microscopy. For viscometry, samples were mixed on ice and 0.5-ml aliquots were transferred to Cannon viscometers at 30°C (Cannon Instruments Co., State College, Pa.). Basal levels of actin assembly were attained by incubating actin at a concentration of 1.0 mg/ml (30°C, 30 min) with 0.4 mM $MgSO_4$ in the buffer (5 mM Tris-HCl, 0.2 mM DTT, 0.1 mM $CaCl_2$, pH 8.0) described by Brenner and Korn (17). As increasing Mg^{+2} concentrations enhance both the rate and extent of actin assembly (17), 2.0 mM $MgSO_4$ was used as a positive assembly control. Drug-induced assembly was studied by incubating either taxol or phalloidin (18) with actin in buffer containing 0.4 mM $MgSO_4$. Specific viscosities (η_{sp}) were calculated as (sample flow time-buffer time)/buffer flow time. Buffer flow times were characteristically 25–26 s. Phalloidin (Boehringer Mannheim Biochemicals, Indianapolis, Ind.) was dissolved in water and taxol in dimethyl sulfoxide.

RESULTS

Taxol Does Not Induce Polymerization of Purified Actin

In questioning the specificity of taxol for MTP, we examined the effect of taxol on the assembly of actin, another in vitro self-assembly system. Purified rabbit muscle actin was incubated with an approximately stoichiometric concentration of taxol (20 μM) under basal assembly conditions (0.4 mM $MgSO_4$) as described in Materials and Methods. As controls, actin assembly was induced by incubation in the presence of 2.0 mM $MgSO_4$ (17) or 20 μM phalloidin (18). Both high magnesium and stoichiometric amounts of phalloidin produce substantial increases in specific viscosity (η_{sp} = 0.57 and 0.43,

[1] Methanol was not used to extract the [^{3}H]taxol from the silica gel because the silica-gel binder is extremely soluble in CH_3OH, and silica itself undergoes a reaction with CH_3OH to produce methyl silicate, which is also soluble in CH_3OH (Dr. Herman Felton, Analtech Corp., Newark, Del., personal communication).

respectively). Taxol did not alter the basal level of actin polymerization (η_{sp} = 0.19). Electron micrographs revealed that, in contrast to the results obtained with either 0.4 mM $MgSO_4$ or taxol, both 2.0 mM $MgSO_4$ and phalloidin induced extensive actin polymerization (data not shown).

[^{3}H]Taxol Binds to Microtubule Protein

[^{3}H]Taxol binding to MTP was examined by the sedimentation assay described in Materials and Methods. In the representative experiment shown here, [^{3}H]taxol, when added before the initiation of assembly, binds to MTP in a saturable manner over two orders of magnitude of drug concentration (Fig. 1 *a*). The reaction produces a hyperbolic binding curve that appears to be first order with respect to ligand concentration in both the presence and absence of GTP. Even at low concentrations of [^{3}H]taxol, binding to MTP appears to be linear (Fig. 1 *b*). A double reciprocal plot of the binding data (Fig. 1 *a*, *inset*) reveals an apparent binding constant, K_{app}, of 0.87 and 0.79 μM and a calculated maximal binding ratio, B_{max}, of 0.60 and 0.54 mol of taxol bound/mol of tubulin dimer (assuming 70% purity) for the plus GTP and the minus GTP experiments, respectively. Although the specific activities of [^{3}H]taxol binding to MTP are similar in the presence and absence of GTP, the presence of GTP enhances the total amount of protein sedimented at steady state (Table I). At the highest concentration of taxol used, GTP no longer increases the amount of protein sedimented. Similar binding experiments with PC-tubulin (≥98% purity) done in the presence of 1 mM GTP results in saturable binding curves with a similar K_{app} and a calculated B_{max} of 0.78 mol taxol bound/mol of tubulin dimer (Fig. 2). With both MTP and PC-tubulin, binding saturation occurs at approximate stoichiometry with the tubulin dimer concentration.

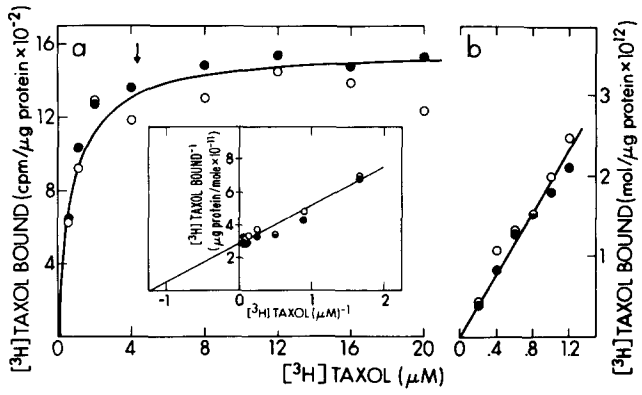

FIGURE 1 (*a*) [^{3}H]Taxol binds to calf-brain MTP in the presence and absence of exogenous GTP. MTP (0.48 mg/ml) was incubated at 37°C with various concentrations of [^{3}H]taxol in the presence (●) and absence (○) of 1 mM GTP. After 60 min, the reaction mixture was layered on 50% sucrose in MES buffer and centrifuged, and the pellets were analyzed for radioactivity and protein as described in Materials and Methods. The binding curve was obtained by fitting all the data to the Michaelis-Menten equation (correlation coefficient, r = 0.97) using a hyperbolic regression analysis package in an Apple II computer. The K_{app} and B_{max}, so calculated, have the same values as when calculated by double reciprocal plot. The arrow denotes the approximate tubulin concentration (μM). *Inset:* double reciprocal plot of the above data is the calculated linear regression line for both experiments yielding a K_{app} of 0.84 μM and B_{max} of 0.56 mol taxol/mol polymerized tubulin. Analysis of the data for the plus and minus GTP experiments individually yields a K_{app} of 0.87 and 0.79 μM and a B_{max} of 0.6 and 0.54 mol taxol/mol polymerized tubulin, respectively. (*b*) Binding of low concentrations of [^{3}H]taxol to MTP in the presence and absence of exogenous GTP. MTP (0.51 mg/ml) was incubated under conditions identical to that in *a*. The scale of the ordinates in *a* and *b* are identical and expressed as cpm/μg at the left ordinate and mol/μg at the right ordinate.

TABLE I

GTP Enhances the Mass of Pelleted Microtubule Polymer in the Presence of [^{3}H]Taxol

	Additions	
[^{3}H]Taxol	+GTP	−GTP
μM	μg protein/aliquot	
0	5.8	≤0.1
0.6	7.4	2.2
1.2	8.9	4.4
2.0	7.5	4.3
4.0	8.5	5.0
8.0	8.8	6.6
12.0	9.0	5.9
16.0	10.5	8.3
20.0	9.3	9.3

Data are from the experiments shown in Fig. 1 a. Protein mass represents the average of duplicate 50-μl aliquots from each pellet.

When drug-treated samples, before sedimentation, were examined by electron microscopy, in the case of both MTP and PC-tubulin, [^{3}H]taxol had induced formation of MTs, hoops, and ribbons, with MTs representing the major polymer form (Figs. 3 and 6 *a*). Although the ratio of hoops, ribbons, and MTs has not been quantified, we estimate that hoops and ribbons represent <10% of the total tubulin polymer population. The average length of the MTs decreased with increasing drug concentration. These findings are in agreement with those of Schiff et al. (2).

Effects of Taxol, Podophyllotoxin, and Vinblastine on [^{3}H]Taxol Binding to Microtubule Protein

As expected, unlabeled taxol added to a MT assembly reaction before initiation competes with [^{3}H]taxol for binding to MTs (Fig. 4) and, as was shown in Table I, polymer mass increases in parallel with the taxol concentration. Podophyllotoxin and vinblastine, drugs that inhibit MT assembly, reduce the specific activity of [^{3}H]taxol binding to sedimentable structures, the latter being more potent (Fig. 4). With both drugs, sedimentable polymer mass is diminished (data not shown). VP-16-213, a congener of podophyllotoxin that does not inhibit MT assembly (19), has no effect on [^{3}H]taxol binding.

Grids for electron microscopy were prepared from reaction mixtures before sedimentation into 50% sucrose. [^{3}H]Taxol (2 μM) assembled MTP into the expected MTs, hoops, and ribbons (Fig. 5 *a*). At equimolar vinblastine, [^{3}H]taxol is unable to promote the formation of any MTs, whereas vinblastine-induced spiral structures are abundant (Fig. 5 *c*). In contrast, podophyllotoxin, at tenfold molar excess, does not completely inhibit taxol-induced MT formation, as very short MTs and ribbons are present at the end of the reaction period (Fig. 5 *b*). Examination by electron microscopy of unsonicated, resuspended pellets showed that the taxol- and the taxol-podophyllotoxin-treated samples contained MTs, ribbons, and neurofilaments, whereas vinblastine-treated samples contained amorphous protein and neurofilaments (data not shown).

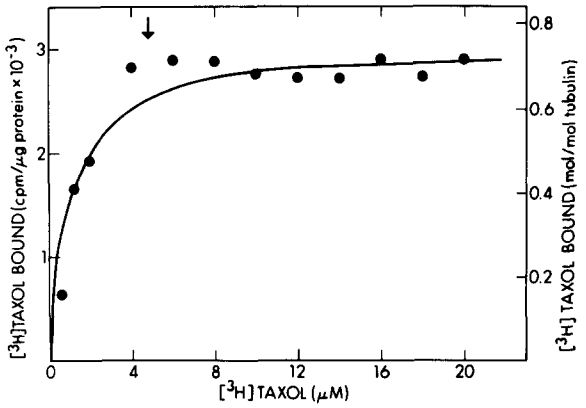

FIGURE 2 [^{3}H]Taxol binds to phosphocellulose-purified tubulin. Tubulin (0.53 mg/ml) was incubated at 37°C with various concentrations of [^{3}H]taxol in MES buffer containing 1 mM GTP. After 60 min, the reaction mixtures were centrifuged through 50% sucrose and the pellets were analyzed for radioactivity and protein as described in Materials and Methods. The results, expressed as cpm/μg protein at the left ordinate and as moles of drug/mole of polymerized tubulin at the right ordinate, are the average of duplicate determinations. The line is a computer-fit rectangular hyperbola, obtained as described in Fig. 1 *a*, yielding a K_{app} of 1.2 μM and B_{max} of 0.78 mol taxol/mol polymerized tubulin. The arrow denotes the approximate tubulin concentration (μM).

[^{3}H]Taxol Binds to Steady State Microtubules

The observation that GTP enhanced the amount of sedimented MTP but not the specific activity of [^{3}H]taxol binding to MTs suggested that taxol binds to polymer. To determine whether [^{3}H]taxol would bind to polymerized MTs, MTP was assembled to steady state in the presence of GTP or GPCPP, a GTP-analog reported to inhibit MT treadmilling (20), and the resulting MTs, resuspended in warm buffer containing [^{3}H]taxol and the nucleotide present during assembly, bound drug with stoichiometries similar to those obtained when MTs were assembled in the presence of tritiated drug (Table II, *B*). Since significantly more protein was sedimented (25% ± 11, n = 3) when assembly took place in the presence of GPCPP instead of GTP (20), resuspension of GPCPP-MTs in less than saturating concentrations of [^{3}H]taxol (2 μM) resulted in a reduction of specific activity. However, when MTs were resuspended in the presence of saturating [^{3}H]taxol concentrations (10 μM), little difference in binding stoichiometry was noted. The binding of [^{3}H]taxol to resuspended MTs is inhibited by unlabeled drug. [^{3}H]Taxol added directly to a solution of steady state MTs (GTP- or GPCPP-assembled) was bound as efficiently as it was during assembly (Table II, *A*).

In a variation of this experiment, MTs assembled in the presence of [^{3}H]taxol were harvested and resuspended in the presence of unlabeled drug. These pellets proved to be sticky and did not disperse well, giving erratic results. Despite the latter problem, our experiments demonstrate that [^{3}H]taxol is able to bind specifically to steady state MTs.

Effect of Taxol, Podophyllotoxin, Vinblastine, and $CaCl_2$ on [^{3}H]Taxol Binding to Steady State Microtubules

The nature of the taxol binding site on the assembled MT was further examined by assembling MTP with either 2 or 10 μM [^{3}H]taxol (below and above saturation, respectively) in the presence of 1 mM GTP at 37°C for 30 min, and by adding various drugs or 4 mM $CaCl_2$ directly to the assembly mixtures. The reaction mixtures were incubated for an additional 30 min at 37°C and sedimented through 50% sucrose. The results are presented in Table III.

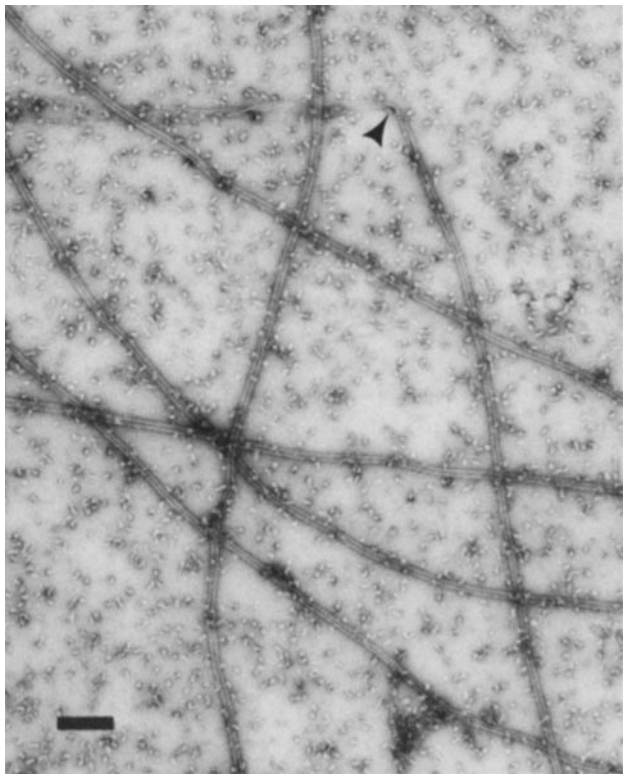

FIGURE 3 MTs assembled from phosphocellulose-purified tubulin in the presence of taxol and GTP. An electron micrograph of MTs assembled from PC-tubulin (4.8 μM) in the presence of GTP (1 mM) and taxol (4 μM) from the experiment shown in Fig. 2. MTs are the primary polymer form, with an occasional ribbon attached to a MT, as seen at the arrowhead. Free ribbon structures also can be found but are not seen in this micrograph. Bar, 0.2 μm. × 36,400.

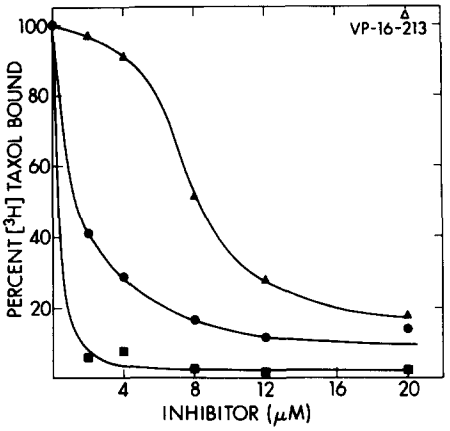

FIGURE 4 Podophyllotoxin, vinblastine, and unlabeled taxol reduce the specific activity of [^{3}H]taxol binding to MTP. Various concentrations of podophyllotoxin (▲), VP-16-213 (△), vinblastine (■), and unlabeled taxol (●) were incubated with 2 μM [^{3}H]taxol, MTP (0.4 mg/ml), and 1 mM GTP at 37°C for 60 min before sedimentation into 50% sucrose. Values are the average of duplicate determinations per pellet. Binding obtained in the presence of [^{3}H]taxol alone (cpm/μg protein) represents a value of 100%.

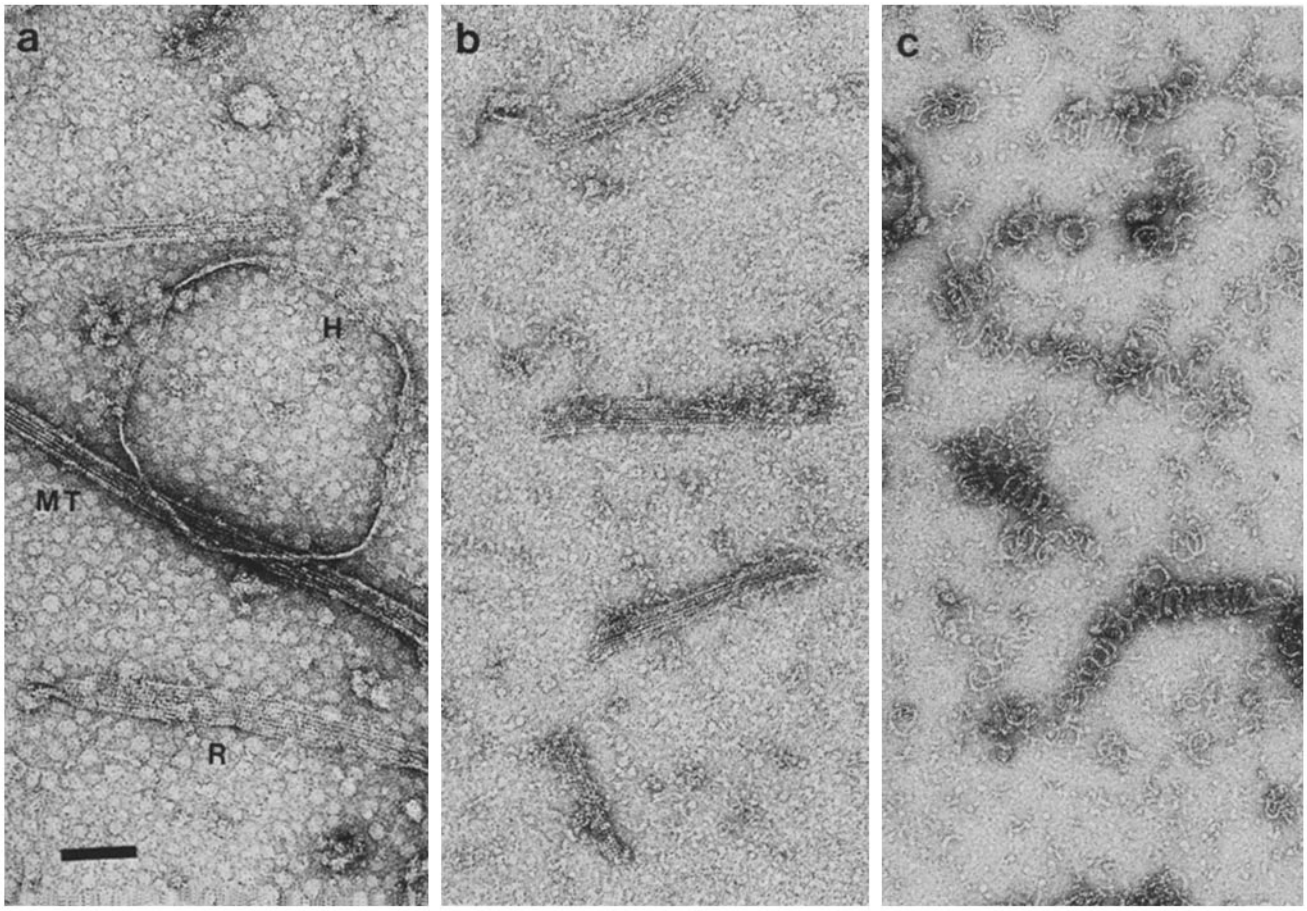

FIGURE 5 Electron micrographs of the 60-min reaction mixtures before sedimentation from the experiment shown in Fig. 4. (*a*) Assembly in the presence of 2 μM [^{3}H]taxol yields predominantly MTs. Hoops (*H*) and ribbons (*R*) represent <10% of the tubulin polymer. (*b*) Assembly in the presence of 2 μM [^{3}H]taxol and 20 μM podophyllotoxin. Note the extremely short MTs and ribbons. (*c*) Assembly in the presence of equimolar concentrations (2 μM) of [^{3}H]taxol and vinblastine. Only vinblastine-induced spiral coils are seen. Bar, 0.1 μm. × 99,000.

Unlabeled taxol displaces [^{3}H]taxol in a concentration-dependent manner. At 2 μM [^{3}H]taxol, both vinblastine and podophyllotoxin decrease the specific activity of [^{3}H]taxol binding to a small degree. This inhibition does not appear to be concentration dependent. However, at 10 μM [^{3}H]taxol, these drugs have less effect on the specific activity of binding. VP-16-213 and $CaCl_2$ do not alter [^{3}H]taxol binding. Both vinblastine and podophyllotoxin were able to effect a decrease in the mass of taxol-assembled MTs sedimented. Thus, both podophyllotoxin and vinblastine directly affect the taxol-stabilized MT polymer, causing either a partial depolymerization or formation of a non- or less-sedimentable polymer.

Examination of electron micrographs from grids prepared before sedimentation revealed that in the case of podophyllotoxin there were fewer and shorter MTs than in the [^{3}H]taxol control (Fig. 6 *a* and *b*), but hoops and ribbons persisted (Fig. 6 *d*). In the vinblastine-treated sample, we were able to visualize many MTs existing side by side with vinblastine-induced coils (Fig. 6 *c*), many of these actually peeling off the MT ends (Fig. 6 *e*). Occasionally, we observed what appeared to be a coil having stripped down the side of a MT (Fig. 6 *e*). Such MTs persisted for at least 3 h, with coils continually growing from MT ends. In contrast, GTP-assembled MTs essentially disappeared within the first 15 min of incubation with vinblastine. Podophyllotoxin added to GTP-assembled MTs caused a decrease in the number and length of MTs but the rate of loss was not so great as with vinblastine. VP-16-213 had no effect on GTP-assembled or taxol-assembled MTs; $CaCl_2$ (4 mM) added to GTP-assembled MTs caused typical ring formation (21) but had no effect on taxol-assembled MTs.

DISCUSSION

Previous reports from our laboratory (2, 3) indicated that taxol induced the assembly of both calf-brain MTP and PC-tubulin. Since, in the former case, it did so in the presence or absence of GTP and, in the latter, in the absence of microtubule-associated proteins (MAPs), we inferred that the activity of taxol was dependent on its ability to bind to tubulin. We prepared biologically active [^{3}H]taxol to directly probe the interaction of the drug with MTP and PC-tubulin. We hoped to determine definitively the macromolecular entity to which taxol binds and describe the parameters of this interaction.

The specificity of the interaction of taxol with tubulin is delineated by our observations that taxol does not assemble actin; additionally, it does not bind to calf thymus DNA. (J. Parness, S. N. Roy, and S. B. Horwitz, unpublished observations). Inasmuch as neurofilaments are the only discrete structures found in the sucrose pellet after combined treatment of MTP with vinblastine and [^{3}H]taxol, and since little or no label is associated with this pellet, it is apparent that neurofilaments also do not bind taxol. Our sedimentation data clearly indicate

that [^{3}H]taxol assembles and binds to tubulin. Unlabeled taxol competes with [^{3}H]taxol when added before assembly and competitively displaces label from assembled MTs. Our experiments with GPCPP, the GTP analog reported to inhibit microtubule treadmilling (20), indicate that [^{3}H]taxol binds to steady-state MTs with stoichiometries similar to those observed when MTs are assembled in the presence of drug. Thus our studies demonstrate that taxol binds specifically and reversibly to tubulin, and that an exposed binding site exists on the intact MT.

The results presented here support the idea that 1 mol of taxol binds per mol of polymerized tubulin dimer. We find that [^{3}H]taxol binds to MTP with a calculated mean B_{max} of 0.6 mol taxol/mol tubulin dimer ($n = 4$). The calculated B_{max} for PC-tubulin, which we know is >98% pure, is 0.78 mol taxol/mol polymerized tubulin dimer. In the case of both PC-tubulin and MTP, binding saturation occurs at approximate stoichiometry with the tubulin dimer concentration. All other known effects of taxol on MTs in vitro have their maxima at concentrations approximately stoichiometric with the tubulin dimer concentration (2, 4). It should be noted that measured maximal binding stoichiometries for drugs such as colchicine have been in the range of 0.5–0.65 (22, 23, 24), and these values have been interpreted to represent one binding site per tubulin dimer.

The observed critical concentration and lag time in GTP-induced MT assembly has been described (25, 26, 27) as evidence for nucleation, the positively cooperative event that must take place before polymer elongation can occur (28). Taxol decreases the critical concentration and lag time for assembly of both MTP and PC-tubulin (2, 3), evidence suggesting that taxol is assisting in the allosteric transition of receptor from the dimeric, nonpolymerized state to the poly-

TABLE II

Binding of [^{3}H]Taxol to Steady State Microtubules Assembled in the Presence of GTP or GPCPP

	dpm/μg protein	% control
A. Addition of [^{3}H]taxol to steady state MTs in solution		
2 μM [^{3}H]taxol		
Control assembly in GTP + [^{3}H]taxol	2,426 ± 208 ($n = 4$)	100
Control assembly in GPCPP + [^{3}H]taxol	2,203 ± 289 ($n = 4$)	91
Assembly in GTP; [^{3}H]taxol added at steady-state	2,507 ± 265 ($n = 4$)	110
Assembly in GPCPP; [^{3}H]taxol added at steady-state	2,394 ± 267 ($n = 4$)	99
B. Resuspension of MTs in [^{3}H]taxol		
2 μM [^{3}H]taxol		
Control assembly in GTP + [^{3}H]taxol	2,176 ± 267 ($n = 4$)	100
Control assembly in GPCPP + [^{3}H]taxol	1,959 ± 87 ($n = 4$)	90
GTP-MTs resuspended in [^{3}H]taxol	2,060 ± 76 ($n = 4$)	95
GTP-MTs resuspended in [^{3}H]taxol + 40 μM unlabeled taxol	252 ± 16 ($n = 2$)	12
GPCPP-MTs resuspended in [^{3}H]taxol*	1,363 ± 53 ($n = 4$)	63
GPCPP-MTs resuspended in [^{3}H]taxol + 40 μM unlabeled taxol	174 ± 10 ($n = 2$)	8
10 μM [^{3}H]taxol		
Control assembly in GTP	3,611 ± 82 ($n = 2$)	100
GTP-MTs resuspended in [^{3}H]taxol	2,965 ± 81 ($n = 4$)	82
GPCPP-MTs resuspended in [^{3}H]taxol	3,316 ± 148 ($n = 6$)	92

MTs were assembled from MTP (0.9 mg/ml) at 37°C, 30 min, in the presence of 1 mM GTP or GPCPP. In A, [^{3}H]taxol was added directly to each assembly mixture and incubated for 30 min at 37°C before sedimentation through 50% sucrose as described in Materials and Methods. In B, MTs were harvested by centrifugation (39,000 × g, 25°C, 30 min) and were resuspended in warm MES buffer containing [^{3}H]taxol and the nucleotide present during assembly. Incubation continued for 30 min at 37°C before centrifugation through 50% sucrose. Pellets were analyzed for radioactivity and protein. Binding observed after assembly with GTP and [^{3}H]taxol is designated as 100%.

* Upon resuspension of MTs assembled with GPCPP, more protein (25 ± 11%, $n = 3$) was present than in the GTP-resuspended reactions.

TABLE III

Effect of Taxol, Vinblastine, Podophyllotoxin, VP-16-213, or $CaCl_2$ on Steady State Microtubules Assembled in the Presence of [^{3}H]Taxol

Additions	Protein	Sp act	Control
	cpm	μg	cpm/μg	%
2 μM [^{3}H]taxol				
None	9,247	6.76	1,368	100
Taxol				
2 μM	4,453	7.74	575	48*
20 μM	953	8.22	116	10*
Vinblastine				
2 μM	4,830	4.54	1,064	78
20 μM	4,095	3.82	1,072	78
Podophyllotoxin				
2 μM	5,247	4.65	1,128	83
20 μM	4,856	4.37	1,111	81
VP-16-213				
20 μM	9,004	6.33	1,422	104
$CaCl_2$				
4 mM	11,617	8.02	1,449	106
10 μM [^{3}H]taxol				
None	14,809	8.24	1,710	100
Vinblastine				
20 μM	7,038	4.28	1,646	96
100 μM	3,609	2.47	1,460	85
Podophyllotoxin				
20 μM	7,839	4.72	1,663	97
100 μM	7,298	4.49	1,627	95

MTs were assembled from MTP (0.43 mg/ml) in the presence of [^{3}H]taxol and 1 mM GTP at 37°C for 30 min. At steady state, drugs were added and incubation was continued for 30 min. After sedimentation through 50% sucrose, pellets were processed for radioactivity and protein as described in Materials and Methods. Results represent the average (±5%) of duplicate 50-μl aliquots.

* Corrected for increase in sedimented MT mass, due to promotion of additional MT assembly by unlabeled taxol.

FIGURE 6 Electron micrographs of steady state MTs assembled in the presence of [^{3}H]taxol and treated with podophyllotoxin and vinblastine. After assembly in the presence of 10 μM [^{3}H]taxol for 30 min (*a*), MTs were treated with 100 μM podophyllotoxin (*b*) or 100 μM vinblastine (*c*) for 30 min. Podophyllotoxin-treated samples contained hoops and ribbons as well as MTs (*d*). Vinblastine-treated samples (*e*) contained MTs and spiral coils. Arrowheads are directed at points of apparent continuity between MTs and vinblastine-induced spiral coils. Bars: *a–c*, 0.1 μm; *d–e*, 0.4 μm. *a–c*, × 25,000; *d–e*, × 99,000.

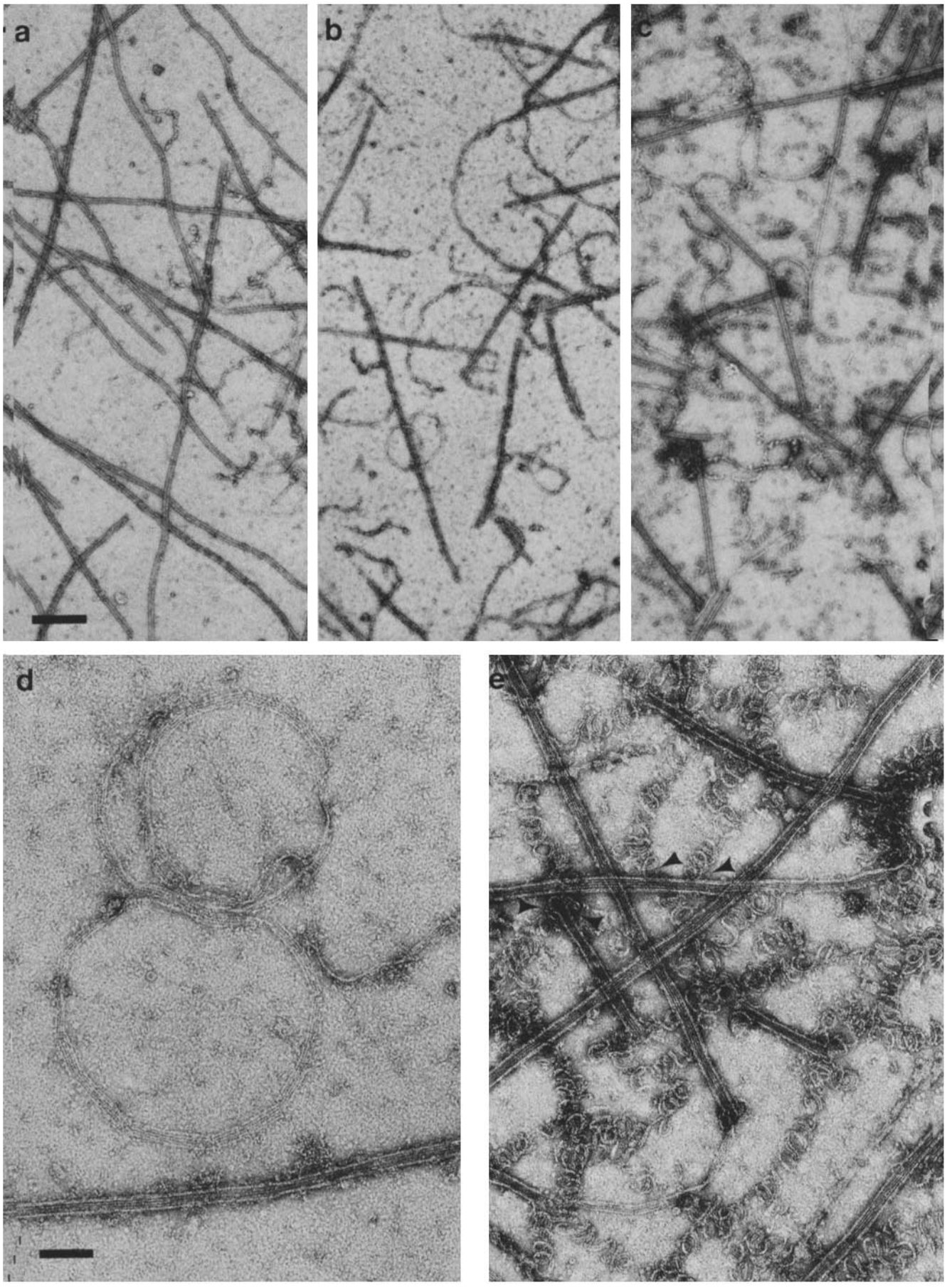
a
b
c
d
e

meric state. We reasoned, therefore, that a model that describes taxol binding might also describe MT assembly, especially as regards nucleation. Yet low concentrations of ligand incubated with MTP produced no detectable sigmoidicity in the taxol binding curve in either the presence or absence of GTP. Evidence that taxol is not changing the initiation of MT assembly into a noncooperative event is that taxol incubated with PC-tubulin, at or below stoichiometry with the drug concentration, promotes assembly only after a lag time (3).

Analysis of our binding experiments by a computer-fit hyperbolic regression program gives excellent fit to the Michaelis-Menten equation until just before binding saturation. Subsequent observed saturation values fall below the calculated line. Goodness of fit to the Michaelis-Menten equation at low ligand (below saturation) but not at high ligand (above saturation) concentrations is consistent with more rapid dissociation of label from pelleting structures at high ligand concentrations, i.e., negative cooperativity or half-of-the-sites reactivity (29). However, linear or slightly convex double reciprocal plots such as shown in Fig. 1 *a* (*inset*) are inconsistent with such a model (30). As noted above with PC-tubulin, the calculated maximal binding ratio is 0.78 mol taxol/mol polymerized tubulin. If one calculated the B_{max} from double reciprocal plots instead of from hyperbolic regression analysis, the value obtained is ~0.95 (data not shown). This discrepancy between the observed and calculated values for PC-tubulin is greater than that seen with MTP and indicates that a hyperbolic binding model may be insufficient to describe the taxol-tubulin interaction. Saturation binding experiments must be carefully controlled to maintain equilibrium conditions to be interpreted correctly (30). The sedimentation assay used in this study represents a removal from equilibrium and signifies the inadequacies of our assay in determining a binding model for taxol. A kinetic as well as a true equilibrium assay must be developed to properly examine the interaction of taxol with tubulin.

Kinetic experiments (12, 31–37) have demonstrated that dilution-, Ca^{+2}-, vinblastine-, and podophyllotoxin-induced MT depolymerization is consistent with an end-dependent mechanism. Whereas MTs assembled in the presence of taxol concentrations greater than or equal to tubulin dimer concentrations are stable upon fivefold dilution (3), it has been postulated that taxol stabilizes MTs by decreasing the net tubulin dissociation constant at the MT ends. Adding MT-depolymerizing drugs to taxol-stabilized steady state MTs does not significantly alter the specific activity of taxol bound to MTs. These drugs do decrease the yield of sedimented protein, an effect not seen with either $CaCl_2$ or VP-16-213. High concentrations of podophyllotoxin and vinblastine, though sufficient to substantially or completely depolymerize GTP-assembled MTs, affect the taxol-stabilized MT to a much lesser degree. Warfield and Bouck (36) observed the peeling off of vinblastine-induced spiral coils from MT ends. Visualization of vinblastine-induced spiral coils peeling off of the ends of taxol-stabilized MTs emphasizes both the end depolymerizing action of vinblastine (36, 37) as well as the relative resistance of the taxol-stabilized ends to undergo depolymerization or major conformational changes. These results are consonant with the stabilization of MTs by taxol through a reduction in the rates of dissociation at the MT ends. We do not know whether vinblastine-induced spiral coils bind taxol as these structures do not sediment in the conditions of our experiments.

When all additions are made before the initiation of assembly, unlabeled taxol specifically dilutes out [^{3}H]taxol binding to tubulin, simultaneously increasing polymer mass by promoting the formation of MTs and other polymeric structures. The effects of podophyllotoxin and vinblastine under similar conditions are more complicated. It is clear that both podophyllotoxin and vinblastine inhibit taxol binding to MTP as a function of the ability of these drugs to alter MT formation, as well as to destabilize existing structures. Vinblastine totally inhibits MT polymer formation in the presence of taxol and inhibits [^{3}H]taxol binding. Podophyllotoxin, even at a tenfold molar excess to the [^{3}H]taxol concentration, is unable to completely inhibit taxol-induced polymer formation and hence is a less potent inhibitor of [^{3}H]taxol binding. If podophyllotoxin inhibits the formation of polymer, thereby proportionately inhibiting the amount of [^{3}H]taxol bound, the specific activity of labeled drug bound to sedimented structures should be unaltered. This is not the case and we suspect at least two reasons. As podophyllotoxin decreases polymer mass, the proportion of the pellet consisting of neurofilaments and aggregated protein increases. This can be a factor in the observed decrease in specific activity. Moreover, if taxol induces podophyllotoxin-tubulin co-polymer formation (colchicine-tubulin co-polymers have been described [38]), the co-polymer may have a lower affinity for taxol. This would lead, in a concentration-dependent manner, to a loss in the specific activity of [^{3}H]taxol binding. Since the action of these drugs in inhibiting taxol binding to tubulin parallels their actions as inhibitors of taxol-induced polymerization, we suggest that podophyllotoxin and vinblastine compete with taxol for interconvertible conformational states of tubulin. Recent experiments by Schiff and Horwitz (3) demonstrate that, in assembly buffer, taxol is a noncompetitive inhibitor of [^{3}H]colchicine binding to tubulin, results which are consistent with the above hypothesis.

Our results with taxol indicate that the action of this drug is specific for the MT system. Taxol causes the formation of cold-stable, abnormal MT bundles in HeLa and 3T3 cells (5, 24) and has been found to promote abnormal MT formations in mouse dorsal root ganglion-spinal cord cultures (39) and aster-like formations in *Xenopus laevis* oocytes (40). In the trypanosome *Trypanosoma cruzi*, taxol inhibits cytokinesis, possibly the result of the freezing of the subpellicular network of MTs, yet duplication of cellular organelles continues (41). We have demonstrated that [^{3}H]taxol binds to MTP in the absence of exogenous guanine nucleotides or in the presence of GTP or GPCPP. It also binds to PC-tubulin in the presence of GTP. With both MTP and PC-tubulin, [^{3}H]taxol binds with a stoichiometry approaching one. The total amount of taxol bound correlates with the mass of MTs formed. The steady state microtubule has a binding site for [^{3}H]taxol, and drug binding is reversible. Once MTs are assembled, bound taxol is as resistant to displacement by MT-depolymerizing drugs or $CaCl_2$ as the MT is resistant to depolymerization. MT inhibitors and taxol involve the tubulin dimer in a set of competing reactions. Hence, when the tubulin dimer is incubated with both taxol and a MT-inhibiting drug, the ultimate polymer state will depend upon the relative affinity of these drugs for the dimer or the dimer-dimer association. Preliminary evidence suggests that under nonpolymerizing conditions [^{3}H]taxol does not bind with high affinity to the tubulin dimer.

[^{3}H]Taxol offers a probe for further delineation of the various states of tubulin involved in MT assembly in vitro and in cells.

We are indebted to G. A. Orr, P. B. Schiff, R. M. Burger, F. Gaskin, J. Peisach, A. Lalezari, J. Condeelis, J. Fant, F. Macaluso, S. Geosits,

and J. J. Manfredi for advice and assistance.

This investigation was supported in part by National Institutes of Health (NIH) grants GM 29042 and CA 15714, and American Cancer Society grant CH-86A. J. Parness is supported by NIH training grant 2T32 GM07260 from the National Institute of General Medical Science.

Received for publication 15 April 1981, and in revised form 10 July 1981.

REFERENCES

1. Wani, M. C., H. L. Taylor, M. E. Wall, P. Coggon, and A. T. McPhail. 1971. Plant antitumor agents. VI. The isolation and structure of taxol, a novel antileukemic and antitumor agent from *Taxus brevifolia*. *J. Am. Chem. Soc.* 93:2325–2327.
2. Schiff, P. B., J. Fant, and S. B. Horwitz. 1979. Promotion of microtubule assembly *in vitro* by taxol. *Nature (Lond.)*. 277:665–667.
3. Schiff, P. B., and S. B. Horwitz. 1981. Taxol assembles tubulin in the absence of exogenous GTP or microtubule associated proteins. *Biochemistry*. 20:3247–3252.
4. Schiff, P. B., and S. B. Horwitz. 1981. Tubulin: a target for chemotherapeutic agents. In Molecular Actions and Targets for Cancer Chemotherapeutic Agents. A. C. Sartorelli, J. S. Lazo, and J. R. Bertino, editors. Bristol-Myers Cancer Symposia, Vol. 2. Academic Press, Inc., N. Y. 483–507.
5. Schiff, P. B., and S. B. Horwitz. 1980. Taxol stabilizes microtubules in mouse fibroblast cells. *Proc. Natl. Acad. Sci. U. S. A.* 77:1561–1565.
6. Shelanski, M. L., F. Gaskin, and C. R. Cantor. 1973. Microtubule assembly in the absence of added nucleotides. *Proc. Natl. Acad. Sci. U. S. A.* 70:765–768.
7. Laemmli, U. K. 1970. Cleavage of structural proteins during assembly of the head of bacteriophage T4. *Nature (Lond.)*. 227:680–685.
8. Kirkpatrick, J. B., L. Hyams, V. L. Thomas, and P. M. Howley. 1970. Purification of intact microtubules from brain. *J. Cell Biol.* 47:384–394.
9. Delacourte, A., M.-T. Plancot, K.-K. Han, H. Hildebrand, and G. Biserte. 1977. Investigation of tubulin fibers formed during microtubule polymerization cycles. *FEBS (Fed. Eur. Biochem. Soc.) Lett.* 77:41–46.
10. Berkowitz, S. B., J. Katagiri, H. K. Binder, and R. C. Williams. Jr. 1977. Separation and characterization of microtubule proteins from calf brain. *Biochemistry*. 16:5610–5617.
11. Weingarten, M. D., A. H. Lockwood, S.-Y. Hwo, and M. W. Kirschner. 1975. A protein factor essential for microtubule assembly. *Proc. Natl. Acad. Sci. U. S. A.* 72:1858–1862.
12. Margolis, R. L., and L. Wilson. 1978. Opposite end assembly and disassembly of microtubules at steady state *in vitro*. *Cell*. 13:1–8.
13. Bradford, M. M. 1976. A rapid and sensitive method for the quantitation of microgram quantities of protein utilizing the principle of protein-dye binding. *Anal. Biochem.* 72:248–254.
14. Lowry, O. H., N. J. Rosebrough, A. L. Farr, and R. J. Randall. 1951. Protein measurement with Folin phenol reagent. *J. Biol. Chem.* 193:265–275.
15. Bensadoun, A., and D. Weinstein. 1976. Assay of proteins in the presence of interfering materials. *Anal. Biochem.* 70:241–250.
16. Asnes, C. F., and L. Wilson. 1979. Isolation of bovine brain microtubule protein without glycerol: polymerization kinetics change during purification cycles. *Anal. Biochem.* 98:64–73.
17. Brenner, S. L., and E. D. Korn. 1979. Substoichiometric concentrations of cytochalasin D inhibit actin polymerization. *J. Biol. Chem.* 254:9982–9985.
18. Wieland, Th. 1977. Modification of actins by phallotoxins. *Naturwissenschaften*. 64:303–309.
19. Loike, J. D., and S. B. Horwitz. 1976. Effects of podophyllotoxin and VP-16-213 on microtubule assembly *in vitro* and nucleoside transport in HeLa cells. *Biochemistry*. 15:5435–5442.
20. Sandoval, I. V., and K. Weber. 1980. Guanosine 5′-(α,β-methylene)triphosphate enhances specifically microtubule nucleation and stops the treadmill of tubulin protomers. *J. Biol. Chem.* 255:6966–6974.
21. Borisy, G. G., and J. B. Olmsted. 1972. Nucleated assembly of microtubules in porcine brain extracts. *Science (Wash., D. C.)*. 177:1196–1197.
22. Weisenberg, R. C., G. G. Borisy, and E. W. Taylor. 1968. The colchicine binding protein of mammalian brain and its relation to microtubules. *Biochemistry*. 7:4466–4478.
23. McClure, W. O., and J. C. Paulson. 1977. The interaction of colchicine and some related alkaloids with rat brain tubulin. *Mol. Pharmacol.* 13:560–575.
24. Schiff, P. B., A. S. Kende, and S. B. Horwitz. 1978. Steganacin: an inhibitor of HeLa cell growth and microtubule assembly *in vitro*. *Biochem. Biophys. Res. Commun.* 85:737–746.
25. Gaskin, F., C. R. Cantor, and M. L. Shelanski. 1974. Turbidimetric studies of the *in vitro* assembly and disassembly of porcine neurotubules. *J. Mol. Biol.* 89:737–758.
26. Borisy, G. G., J. B. Omlmsted, J. M. Marcum, and C. Allen. 1974. Microtubule assembly *in vitro*. *Fed. Proc.* 33:167–174.
27. Lee, J. C., and S. N. Timasheff. 1975. The reconstitution of microtubules from purified calf brain tubulin. *Biochemistry*. 14:5183–5187.
28. Oosawa, F., and M. Kasai. 1962. A theory of linear and helical aggregations of macromolecules. *J. Mol. Biol.* 4:10–21.
29. Koshland, D. E., Jr., G. Némethy, and D. Filmer. 1966. Comparison of experimental binding data and theoretical models in proteins containing subunits. *Biochemistry*. 5:365–386.
30. Boeynaems, J. M., and J. E. Dumont. 1975. Quantitative analysis of the binding of ligands to their receptors. *J. Cyclic. Nucleotide Res.* 1:123–142.
31. Karr, T. L., D. Kristofferson, and D. L. Purich. 1980. Mechanism of microtubule depolymerization. *J. Biol. Chem.* 255:8560–8566.
32. Karr, T. L., D. Kristofferson, and D. L. Purich. 1980. Calcium ion induces endwise depolymerization of bovine brain microtubules. *J. Biol. Chem.* 255:11853–11856.
33. Karr, T. L., and D. L. Purich. 1979. A microtubule assembly/disassembly model based on drug effects and depolymerization kinetics after rapid dilution. *J. Biol. Chem.* 254:10885–10888.
34. Bergen, L. G., and G. G. Borisy. 1980. Head-to-tail polymerization of microtubules in vitro. *J. Cell Biol.* 84:141–150.
35. Summers, K., and M. W. Kirschner. 1979. Characteristics of the polar assembly and disassembly of microtubules observed in vitro by darkfield light microscopy. *J. Cell Biol.* 83:205–217.
36. Warfield, R. K. N., and G. B. Bouck. 1975. Microtubule-macrotubule transitions. Intermediates after exposure to the mitotic inhibitor vinblastine. *Science (Wash., D.C.)*. 186:1219–1221.
37. Himes, R. C., R. N. Kersey, I. Heller-Bettinger, and F. E. Samson. 1976. Action of the *Vinca* alkaloids vincristine, vinblastine and desacetyl vinblastine amide on microtubules *in vitro*. *Cancer Res.* 36:3798–3802.
38. Sternlicht, H., and I. Ringel. 1979. Colchicine inhibition of microtubule assembly via copolymer formation. *J. Biol. Chem.* 254:10540–10550.
39. Masurovsky, E. B., E. R. Peterson, S. M. Crain, and S. B. Horwitz. 1981. Microtubule arrays in taxol-treated mouse dorsal root ganglion-spinal cord cultures. *Brain Res.* 217:392–398.
40. Heidemann, S. R., and P. T. Gallas. 1980. The effect of taxol on living eggs of *Xenopus laevis*. *Dev. Biol.* 80:489–494.
41. Baum, S. G., M. Wittner, J. P. Nadler, S. B. Horwitz, J. E. Dennis, P. B. Schiff, and H. B. Tanowitz. 1981. Taxol, a microtubule stabilizing agent, blocks the replication of *Trypanosoma cruzi*. *Proc. Natl. Acad. Sci. U. S. A.* 78:4571–4575.